Chapter 20
Near-Surface Sensor-Derived Phenology

Oscar R. Zimmerman[1], Andrew. D. Richardson[1,2]

[1]Center for Ecosystem Science and Society, Northern Arizona University, Flagstaff, AZ 86011 USA

[2]School of Informatics, Computing, and Cyber Systems, Northern Arizona University, Flagstaff, AZ 86011 USA

Abstract Near-surface remote sensing provides a novel approach to phenological monitoring. Optical sensors mounted in proximity to the land surface can be used to quantify changes in the spectral properties of vegetation associated with development and senescence, as well as seasonal variation in activity. The resulting data are essentially continuous in time and cover a scale—intermediate between individual organisms and satellite pixels—that is unique and advantageous for a variety of applications. In this chapter, we review and discuss several approaches to near-surface remote sensing of phenology, including methods based on broad- and narrow-band radiometric sensors, and using consumer-grade digital cameras as inexpensive imaging sensors—with an emphasis on what has become known as the "phenocam" method.

20.1 Introduction

Traditionally, plant phenology data have been recorded by a human observer, based on direct visual inspection of individual organisms in the field (e.g., Sparks and Menzel 2002). This approach is suited to the identification of dates at which specific phenophases (e.g., budburst or flowering) occur. The advent of satellite remote sensing in the 1970s opened up new opportunities for global-scale monitoring of seasonal changes in the spectral properties of vegetation. Vegetation indices, such as the normalized difference vegetation index (NDVI) and enhanced vegetation index (EVI), have been used to quantify vegetation greenness, and various algorithms have been developed to estimate the timing of phenological transitions (e.g., start- and end-of-season) from time series of these indices (e.g., Zhang et al. 2018, Bolton et al. 2020).

An alternative to these approaches exists in the form of near-surface remote sensing, in which radiometric or imaging sensors, typically fixed to permanent structures (e.g., towers, masts, or buildings), are used to observe and quantify changes in the land surface in a manner analogous to satellite-based remote sensing, but at a spatial scale similar to ground observations by a human.

ą

One advantage of near-surface remote sensing is its ability to serve as a bridge between direct observations and satellite data, and thus to facilitate scaling from organisms to landscapes. With near-surface remote sensing, spatial integration across the canopy is possible, thereby facilitating comparison with eddy covariance measurements of CO_2 and H_2O fluxes, and simplifying analysis of relationships between phenology and ecosystem processes.

However, there are other reasons why near-surface remote sensing has great potential for routine phenological monitoring. For example, compared to either direct or satellite-based observations, for which data are typically available only at intervals of days to weeks, automated sensors can provide data that are essentially continuous in time.

Additionally, near-surface remote sensing data provide quantitative information about the whole seasonal trajectory of vegetation development and senescence for a well-defined group of organisms within the sensor footprint. By comparison, data collected by a human observer are potentially subjective, and inherently difficult to put on an ordinal scale. Satellite pixels, on the other hand, may integrate across heterogeneous species mixtures or different land cover types, which is valuable for some applications but complicates biological interpretation of the observed seasonal patterns or trends.

Finally, by combining different types of near-surface sensor data, it may be possible to separate seasonal changes in canopy structure from changes in canopy function, especially as related to photosynthetic capacity or efficiency.

In this chapter, we provide an overview of some of the different sensor-based approaches to monitoring phenology. We discuss the instrumentation requirements and data processing, review applications of different technologies, evaluate uncertainties and shortcomings, highlight publicly available datasets and tools, and identify future prospects.

20.2 Instruments for Sensor-based Phenology

Near-surface remote sensing technologies can be divided into two broad categories: radiometric sensors and imaging sensors.

Radiometric sensors vary in their field of view, from wide (up to 180°) to narrow (<45°), and their spectral sensitivity, from broadband to narrowband (Balzarolo et al. 2011). Broadband sensors include the Li-Cor LI-190 quantum sensor to measure photosynthetic photon flux density (PPFD, 400–700 nm) and the Kipp and Zonen CMP-6 pyranometer to measure total shortwave solar radiation (285–2800 nm). Narrowband sensors target specific regions or bands of the electromagnetic spectrum. These range in sophistication from Skye's SKR1800 two-channel sensor with red (625–680 nm) and near-infrared (835–890 nm) bands, to multichannel spectrometers (e.g., ASD, Ocean Optics, or PP Systems) that can simultaneously measure hundreds of bands across an entire spectral range. Each of these sensors outputs a single number that averages across the measurement footprint.

Thus, there is typically no information about spatial variability (but see Tortini et al. 2015) and it is not possible to distinguish among objects or individual organisms within the instrument's field of view.

Imaging sensors, on the other hand, produce digital pictures of a scene with which spatial variability can be analyzed and, if the pictures are of sufficient resolution, different organisms (or even organs) can be identified. These range from consumer-grade digital cameras (including networked cameras or webcams, e.g., StarDot, Axis) that record conventional RGB (red-green-blue) imagery, to hyperspectral cameras that yield information in as many as 128 specific wavebands (e.g., SOC 710, Surface Optics). Highly sophisticated imaging spectrometers, such as HeadWall Photonics' HyperSpec solar-induced fluorescence imager, also fall in this category.

A key distinction between radiometric sensors and most imaging sensors is that the former can be calibrated to yield measurements of radiance (flux density, or power per unit area), whereas the latter usually (imaging spectroradiometers are a noted exception) are not.

Broadband sensors and inexpensive digital cameras have their limitations, but the challenges and expense of more sophisticated instruments also limit the broader use of this technology; ultimately the answer to "what approach is best?" depends on many competing factors, including the science question; the need for accuracy, precision, and traceable calibrations; and the application-specific need for ultrafine-resolution changes in reflected spectral radiance.

20.3 Broadband Radiometric Sensors

The foliage of terrestrial vegetation absorbs most (>80%) incident solar radiation in the visible region (400–700 nm) of the electromagnetic spectrum, because these are the wavelengths that are used to drive photosynthesis. Longer wavelengths in the near-infrared (700–1,400 nm), which are of little use for photosynthesis, are only weakly absorbed. Thus, both transmittance and reflectance of infrared wavelengths tend to be high. The distinction between low reflectance of visible wavelengths, and high reflectance of infrared wavelengths, is a spectral signature that can be used to distinguish healthy green vegetation from soil, branches, and senescent material. This is the basis of the commonly used normalized difference vegetation index (NDVI), where r denotes reflectance:

$$\mathrm{NDVI} = \frac{r_{\mathrm{NIR}} - r_{\mathrm{red}}}{r_{\mathrm{NIR}} + r_{\mathrm{red}}}$$

Huemmrich et al. (1999) noted that readily available broadband sensors could be used to measure quantities that would correspond approximately to r_{red} and r_{NIR}. Specifically, by measuring incident (Q^{-}) and reflected (Q-) PPFD with a

é

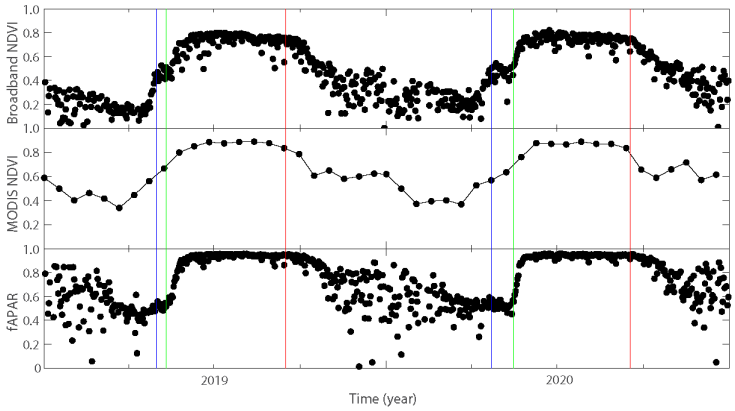

Fig. 20.1 Time series of broadband NDVI, MODIS NDVI, and f_{APAR} at Bartlett Experimental Forest (2019–2020). Broadband indices represent mid-day average values. MODIS data are from the MOD13Q1 product (16-day best available pixel values). Dominant vegetation is comprised of deciduous northern hardwood (maple-beech-birch) species. Snowmelt date (*blue line*), budburst date (*green line*), and onset of autumn leaf coloration (*red line*), based on visual assessment of phenocam imagery from the same tower, are indicated.

quantum sensor, r_{VIS} ($=Q\text{-}/\bar{Q}$) could be used as an estimate of r_{red}. Subsequently, shortwave albedo, calculating from incident ($\bar{R}$) and reflected (R-) solar radiation fluxes measured with upward and downward pointing pyranometers ($\alpha = R\text{-}/\bar{R}$), would provide an estimate of $r_{VIS+NIR}$. Because PPFD is measured in μmol m^{-2} s^{-1}, whereas shortwave solar radiation is measured in W m^{-2}, estimation of r_{NIR} itself requires some assumptions to standardize the units. These assumptions are discussed and evaluated more fully by Huemmrich et al. (1999) and Jenkins et al. (2007). One solution they describe is to estimate r_{NIR} as:

$$r_{NIR} = \frac{R\uparrow - 0.25 \times Q\uparrow}{R\downarrow - 0.25 \times Q\downarrow}$$

Calculated using these estimates of r_{red} and r_{NIR}, "broadband NDVI" has been used to monitor phenology in a number of different vegetation types (Fig. 20.1; Jenkins et al. 2007, Wilson and Meyers 2007, Doughty and Goulden 2008, Wohlfahrt et al. 2010, Liu et al. 2019, Soudani et al. 2021). In many of these studies, broadband NDVI has compared favorably with NDVI calculated from satellite data, with the higher time resolution of broadband NDVI an obvious advantage (see also Fig. 20.1).

In some studies, the broadband NDVI signal has been shown to be noisy during winter months (Fig. 20.1). Furthermore, there is a two-stage rise in NDVI that occurs with snowmelt (stage 1), and green-up (stage 2); failure to identify these as separate events will bias estimates of phenological dates. However, despite these limitations, as well as the assumptions gone into the formulation of

ę

broadband NDVI, the quality of data from spring through summer is generally sufficient to clearly distinguish leaf-on and leaf-off dates, and to track the rates of canopy development and senescence.

Canopy phenology can also be monitored with continuous measurements of photosynthetically active radiation above (Q^{-}, Q-) and below (transmitted, Q_T) the canopy, thereby permitting its absorbed fraction (f_{APAR}) to be calculated (Fig. 20.1; Jenkins et al. 2007, Wohlfahrt et al. 2010, Soudani et al. 2021). Ignoring the radiation that is reflected from the soil or forest floor:

$$\mathrm{APAR} = Q\downarrow - Q\uparrow - Q_T\,;\; f_{APAR} = \frac{\mathrm{APAR}}{Q\downarrow}$$

APAR (absorbed photosynthetically active radiation) may be calculated in a number of different ways, including using mid-day data and daily integrals. However, both methods are subject to the effects of seasonal variation in solar elevation. One solution is to calculate APAR using measurements when the solar zenith angle is closest to 57°—at this angle the fraction of leaf area projected normal to the solar beam converges to one single value across all leaf angle distributions (Myeni et al. 1989), and thus multiple solar angle effects can be controlled for. This latter method is also useful if continuous estimates of leaf area index are to be made from calculated transmittance ($=Q_T/Q^{-}$) using gap fraction theory (Toda and Richardson 2018; see also Rogers et al. 2021).

As with broadband NDVI, snow on upward-pointing sensors can be problematic during winter months (Fig. 20.1). Airborne dust may also in some cases necessitate frequent cleaning of sensors. Finally, spatial heterogeneity in the below-canopy light environment (e.g., sunflecks) can be substantial, and adequate sampling is necessary to reduce uncertainties (Garrity et al. 2011).

20.4 Narrowband Radiometric Sensors

Narrowband radiometric sensors can also be used to measure vegetation indices such as NDVI (e.g., Eklundh et al. 2011, Soudani et al. 2012), and in this application narrowband sensors may be better than broadband sensors (sec. 20.3, above). An advantage to working with narrowband instruments is that the very same wavebands that are used in satellite remote sensing can be targeted. Alternatively, specific wavelengths may be chosen because of their physiological relevance. The photochemical reflectance index (PRI), which tracks diurnal changes in xanthophyll cycle pigments through narrowband reflectance measurements at 531 and 570 nm, is one such example (Gamon et al. 1992, 1997). PRI is also influenced by seasonally changing carotenoid to chlorophyll pigment ratios (or vice-versa), which tend to dominate its annual cycle (Wong and Gamon 2015b). A number of studies have used PRI in the latter sense to monitor seasonal variation

ę

in vegetation function (photosynthetic capacity or efficiency) as opposed to seasonal variation in vegetation structure (development and senescence of leaves) (Wong and Gamon 2015a, Springer et al. 2017, Eitel et al. 2020, Wong et al. 2020). This approach might be especially useful in vegetation types that display large seasonality but remain green year-round. Gamon et al. (2016) developed a closely related chlorophyll/carotenoid index that can be calculated from MODIS wavebands with this objective in mind.

The cost of narrowband instruments, which are targeted at a smaller end-user market, has historically been higher than broadband instruments. Fortunately, low-cost sensors for measuring NDVI and PRI, such as filtered photodiodes, are now commercially available (e.g., Apogee). Other inexpensive alternatives have also been developed and are in use by specific research groups (Ryu et al. 2010, Soudani et al. 2012). As the momentum for open science builds and more papers are published with the details of building and calibrating a specific sensor (e.g., Ryu et al. 2010), we can expect to see more sensors custom-built using off-the-shelf components being used to measure quantities that in the past could only be measured with sensors sold by commercial outfits.

Various tower-mounted spectrometers have been deployed, many of which are specialized, custom-built instruments (Tortini et al. 2015). One application that has been the focus of a number of recently developed instruments is the measurement of solar-induced fluorescence (SIF), a small emission of red and far-red light (650–800 nm) from chlorophyll molecules during sunlight absorption for photosynthesis (Cogliati et al. 2015, Grossmann et al. 2018, Yang et al. 2018). The potential of using SIF to monitor phenology is that seasonal variation in vegetation activity can be directly measured (Magney et al. 2019, Pierrat et al. 2022). However, SIF measurement is a highly sophisticated process relative to the simple calculation of spectral indices. For example, accurate measurements require the use of a spectrometer with high spectral resolution (~0.1–0.3 nm) and high signal-to-noise ratio to retrieve the small fluorescence signal from within narrow absorption bands in the solar spectrum. These include two oxygen absorption bands located at around 687 nm (O_2-B) and 760 nm (O_2-A), as well as several nearby solar Fraunhofer lines. Although there are now some commercially available instruments for continuous monitoring of SIF, such as the "FloX" (JB Hyperspectral Devices), these are still highly specialized instruments with research objectives that usually extend beyond simple monitoring of phenology.

20.5 Monitoring Phenology with Imaging Sensors

The use of standard digital cameras for monitoring phenology has grown substantially over the last dozen years or so, with most studies applying what has become known as the "phenocam" approach (Richardson 2019, 2023). The basic idea of this method is that with timelapse images, taken from a fixed location and with a set field of view and viewing geometry, changes in the characteristics of

í

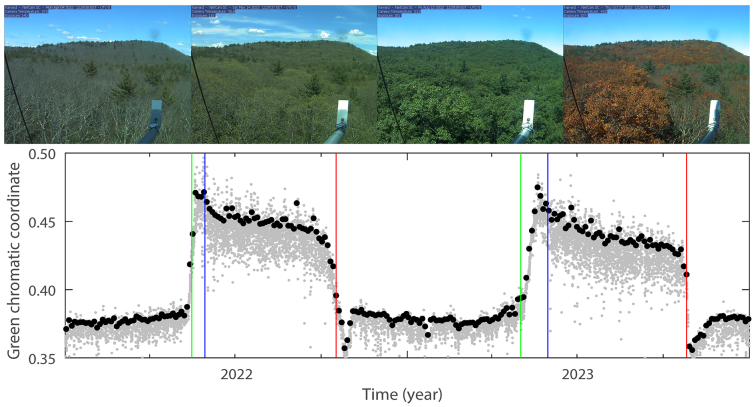

Fig. 20.2 View of the Harvard Forest canopy, from a phenocam mounted on the EMS AmeriFlux tower (*top*), through winter, early spring, summer, and autumn (L to R). The time series of canopy greenness (2022–2023, *bottom*) has been quantified from phenocam images using the green chromatic coordinate. Both raw values from half-hourly images (*small gray circles)* and a summarized 3-day product, calculated using the 90th percentile approach (*large black circles*), are plotted. Ground observations of 50% budburst (*green lines*), 50% of leaves at final length (*blue lines*), and 50% autumn leaf color (*red lines*) are indicated for the dominant species (red oak) in the camera footprint.

vegetation can be detected (Figs. 20.2 and 20.3). This idea is similar to using repeat photographs to track landscape change over decades (e.g., Webb et al. 2003), but is distinguished by the high frequency of image acquisition (one or more images per day) and the emphasis on quantitative data calculated from the images, especially color-based indices (Figs. 20.2 and 20.4; Sonnentag et al. 2012, Richardson et al. 2018a). The annual cycle of canopy greenness derived from camera imagery, for example, clearly reveals information on leaf development and senescence (Fig. 20.2). One advantage of this approach over radiometric measurements is that archived images provide a permanent visual record of what the camera was looking at, at a specific place and time. Visually inspecting the images can be used to validate automated methods of quantifying phenology (Klosterman et al. 2014, Kosmala et al. 2016), or provide information that could help interpret the observed phenological patterns, including establishment, growth, and mortality; disturbance and recovery; and timing and duration of snowpack. The same level of interpretability is not possible with data from non-imaging sensors.

Fig. 20.3 Examples of phenocams installed in the field. (Top left) A camera installed at the University of Michigan Biological Station with an oblique landscape-level view of a deciduous broadleaf forest. (Bottom left) A camera installed near ground level to monitor an experimental plot in a semi-arid grassland at the Sevilleta National Wildlife Refuge, New Mexico. (Right) A camera installed on an instrument tower in a woodland at Cedar Mesa, Utah together with an eddy covariance system (installed directly above at the end of the boom) for measuring canopy-level CO_2 and H_2O fluxes.

20.5.1 Camera Selection

Many different inexpensive and commercially available digital cameras have been used as phenocams (which we define here as any digital camera used for phenological monitoring with the approach described above) (Sonnentag et al. 2012). These include networked cameras or webcams that can be accessed over the Internet, as well as trailcams and point-and-shoot cameras, with prices ranging from $100 to $3,000. Webcams are widely used because the captured images can be viewed and archived off-site in real-time, and system uptime can be remotely verified. Many webcams are stand-alone and thus can operate in the field without additional hardware. In terms of the effect of camera brand and model on the quantitative assessment of phenology, Sonnentag et al. (2012) demonstrated that a number of readily available cameras are suitable for such analyses. However, it is essential that the selected camera has the option to turn off any automatic color or

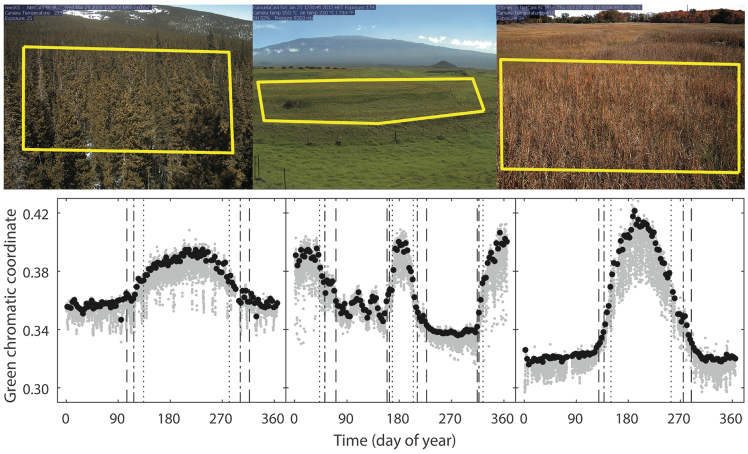

Fig. 20.4 Time series of green chromatic coordinate (g_{CC}) derived from phenocam images captured in diverse ecosystems. Left to right: a subalpine conifer forest at Niwot Ridge, Colorado; a C3/C4 grassland near Kamuela, Hawaii; and a salt marsh at the St. Jones Estuarine Research Reserve, Delaware. The yellow polygons indicate the region of interest analyzed within each image. Phenophase transition dates are calculated from each greenness-rising and -falling stage as the date that the smoothed g_{CC} (spline-fit; not shown) rises above or drops below 10% (*dashed line*), 25% (*dash-dotted line*), or 50% (*dotted line*) of the g_{CC} amplitude for that cycle.

white balancing, which changes the color sensitivity of the RGB (red-green-blue) channels from picture to picture (Seyednasrollah et al. 2019). A camera with minimal or no internal image processing is also desirable, and the acquired images should be of sufficient quality to capture relatively noise-free time series of color-based indices. Lastly, investing in a durable and high-quality camera will overall maximize its lifetime in the field. This is especially crucial if long-term monitoring is a research objective. Several long-running phenocams (including a StarDot NetCam SC that was installed by one of the authors over 15 years ago at Harvard Forest, Fig. 20.2) demonstrate that commercial-grade digital cameras can indeed be used as robust research instruments for long-term monitoring of phenology.

20.5.2 Field Installation

Most phenocams are installed on towers, masts, tripods, or the roofs of field stations, usually at heights taller than the vegetation of interest, with an oblique view that broadly captures the vegetation across the landscape (Figs. 20.2 and 20.3). Phenocams have also been used to monitor individual experimental plots and many are installed alongside other instruments (Fig. 20.3). Cameras should be securely fastened to their mounting structure so that the same field of view and viewing geometry can be kept over time. Otherwise, image masks (de-

áó

scribed in sec. 20.5.3, below) may need to be constantly adjusted, compromising data quality and continuity (Richardson et al. 2018a). Cameras are oriented north (in the northern hemisphere) to minimize lens flare, forward scattering off the canopy, and deep shadows, and pointed somewhat below the horizon to include a mix of both vegetation (~80%) and some sky (~20%). With the exception of automatic exposure, it is recommended that all automatic camera settings be turned off. And while images need not be archived every minute, recording multiple images per day (such as every half hour) increases the likelihood of images being captured under ideal lighting conditions. At sites where there is no previously established Internet connection, a cellular or satellite modem may be used for long-distance telemetry of phenocam imagery.

20.5.3 Image Processing

Almost without exception, current digital cameras use the red-green-blue (RGB) additive color model to represent colors perceived by the human eye. Basically, this means that digital images are comprised of three layers, with each layer corresponding to one of the color channels. For each color channel, there is a two-dimensional array of pixels that represent the image in that color. The resulting color and brightness of a given pixel is then characterized by the intensity of the pixel in each color layer, which is stored as a digital number (DN) triplet. In 24-bit images, there are 8 bits per channel and thus DN values range from 0 to 255.

The first step to processing phenocam imagery involves extracting the DN triplets for individual pixels, and then averaging the DN triplets across multiple pixels within a user-defined region of interest (ROI) (Fig. 20.4). Selecting the ROI depends primarily on the research question being asked; an ROI may correspond to, for example, an individual tree crown, or all trees in the foreground of the images. The pixels corresponding to the ROI are defined by an image mask (a binary array of zeros and ones). Masks may need to be adjusted during the monitoring period to keep the pixels being analyzed consistent, for example, if the camera's field of view shifts over time, or if trees become toppled or defoliated from disturbance.

Time series of RGB DN triplets are noisy and are of little use for phenological analyses because both external factors affecting scene illumination (clouds, aerosols, solar elevation/azimuth) and in-camera image processing (including exposure control) confound the underlying phenological signal. This variability can be largely suppressed by converting the DN triplets (R_{DN}, G_{DN}, B_{DN}) to their respective chromatic coordinates (r_{CC}, g_{CC}, b_{CC}) (Sonnentag et al. 2012, Richardson et al. 2018a). Numerous studies have demonstrated the value of the green chromatic coordinate g_{CC} for characterizing the seasonal trajectory of vegetation color and extracting phenological data. As a result, g_{CC} has become the standard vegetation index calculated from phenocam imagery.

áá

$$r_{CC} = \frac{R_{DN}}{R_{DN} + G_{DN} + B_{DN}}; g_{CC} = \frac{G_{DN}}{R_{DN} + G_{DN} + B_{DN}}; b_{CC} = \frac{B_{DN}}{R_{DN} + G_{DN} + B_{DN}}$$

Even after RGB DN triplets have been converted to chromatic coordinates, substantial variability may remain. One method of extracting the best quality phenological signal is to use a moving-window quantile approach (Sonnentag et al. 2012). This method effectively discards the images taken under sub-optimal conditions, which tend to reduce the observed vegetation greenness (Figs. 20.2 and 20.4). In most cases, the 90th percentile of each chromatic coordinate, extracted from all images collected over a 3-day period, is calculated, and then assigned to the middle day. If outliers persist, other statistical procedures need to be used to clean the data (Richardson et al. 2018a).

Lastly, while there are applications that use the entire annual cycle of calculated canopy greenness, many others are focused only on the timing of specific phenological transitions (e.g., start- and end-of-season dates). Highly flexible spline-based curve fitting methods have been especially useful for quantifying these dates (Richardson et al. 2018a). Transition dates may be determined, for example, as the date that the smoothed g_{CC} rises above or drops below a threshold value, calculated as some percentage (e.g., 10, 25, or 50%) of the g_{CC} amplitude (maximum minus minimum value) for that seasonal cycle (Fig. 20.4).

We note that the approach described above is not the only method of quantifying phenology from repeat digital photographs. Many studies have used variations or extensions of this approach, while others have applied completely different methods. Some examples include pixel-level analyses (Ide and Oguma, 2013), the use of textural metrics (Almeida et al. 2014), and the quantification of flowering phenology using image segmentation and deep learning (Andreatta et al. 2023).

20.5.4 Interpretation and Validation

The seasonal pattern of color-based indices can be mostly explained by the combined effect of two main vegetation characteristics: (1) changes in canopy structure, especially as influenced by leaf development and senescence; and (2) changes in leaf-level traits, particularly those associated with leaf coloration. For example, Keenan et al. (2014) showed using a two-endmember mixing model that the g_{CC} of a deciduous broadleaf forest was directly related to the amount of leaf area present and the color of individual leaves (which was measured on a flatbed scanner). Taking a more mechanistic approach, Wingate et al. (2015) were able to simulate the seasonal trajectory of all three chromatic coordinates (r_{CC}, g_{CC}, and b_{CC}) by adjusting levels of leaf area index and the sizes of several major pigment pools within a radiative transfer model. The ability of color-based indices to represent aspects of both canopy structure and seasonal physiology makes it possible to

áą

quantify a range of phenological phenomena, across many different vegetation types, from phenocam imagery. Examples include dates of leaf development, autumn coloration, and leaf drop, to seasonal variation in photosynthetic capacity and vegetation activity, particularly canopy-level CO_2 fluxes (Keenan et al. 2014, Klosterman et al. 2014, Toomey et al. 2015, Kosmala et al. 2016, Bowling et al. 2018, Seyednasrollah et al. 2021).

20.5.5 Camera Networks, Open-source Data, and Applications

Networks of digital cameras enable phenology to be monitored across multiple sites that cover gradients in climate and vegetation. For example, many researchers maintain mesonets of cameras within a specific geographic region. Several continental-level camera networks have also been established. These include a Phenological Eyes Network (Nasahara and Nagai 2015), European Phenology Camera Network (Wingate et al. 2015), Australian Phenocam Network (Brown et al. 2016), and a PhenoCam Network made up of 700+ cameras across North America and the greater globe (Richardson 2023). The archive of PhenoCam imagery is publicly available and updated in real time. Anyone can contribute to the network but must follow a standard protocol, such as the use of a standard camera and configuration. For each site, PhenoCam also processes the imagery (extraction of color-based indices and calculation of transition dates) and makes that data publicly available (Richardson et al. 2018a). These datasets are suited for a variety of applications, including the evaluation of satellite remote sensing products (Richardson et al. 2018b, Moon et al. 2021), phenological model development and testing (Seyednasrollah et al. 2021, Post et al. 2022, Schädel et al. 2023), and investigating relationships between phenology and ecosystem processes (Young et al. 2021, 2022). Many sites are a part of other research networks (e.g., FLUXNET, NEON), thus facilitating the integration of PhenoCam data with other co-located observations. All PhenoCam imagery and datasets can be accessed from the PhenoCam website (https://phenocam.nau.edu) or obtained from the curated and documented data releases (Richardson et al. 2018a, Seyednasrollah et al. 2019, Young et al. *in preparation*). A list of open-source tools for customized image analyses and interacting with the archive of PhenoCam data can also be found online (https://phenocam.nau.edu/webcam/tools/).

20.5.6 Other Possibilities with Imaging Sensors

Conventional digital cameras can be used in a number of other configurations for phenological monitoring. For example, fisheye (180°) lenses have been used to record hemispherical photographs of vegetation from nadir (Nasahara and Nagai 2015), or from beneath the canopy pointing directly upward (Toda and

Richardson 2018, Brown et al. 2020). Upward- and downward-looking images can be analyzed to estimate leaf area index using gap fraction theory (Ryu et al. 2012, Liu et al. 2013). Cameras can also be installed close-up to specific plants for visual assessment of phenology at the bud-to-branch scale, or on mobile platforms, such as remotely piloted aircraft systems, for extrapolation across the landscape (Klosterman et al. 2018, Atkins et al. 2020).

The imaging sensors in most conventional digital cameras are sensitive to infrared radiation (700–1000 nm). A cut filter over the sensor normally blocks these wavelengths, but this filter can be removed altogether, resulting in composite RGB + IR images. Some cameras allow the IR filter to be triggered, enabling back-to-back RGB and RGB + IR images to be recorded (Fig. 22.5). Petach et al. (2014) leveraged this capability to calculate "camera NDVI", and their method has since been incorporated into the PhenoCam Network's standard protocol (Young et al. *in preparation*). To test the utility of the added information, Filippa et al. (2018) compared the seasonal trajectories of g_{CC} and camera NDVI in a number of different vegetation types. At most sites, the two patterns were overall comparable, with slight lags and slightly lower signal-to-noise ratio in NDVI (see also Fig. 22.5). In evergreen vegetation, the difference was greater, with NDVI being more sensitive to the formation of new needles and seed cones than g_{CC}, which was more indicative of canopy color. Camera NDVI was thus concluded to be complementary (rather than redundant) to color-based indices, and there may be use cases where camera NDVI would be favored over g_{CC}. One example is the evaluation of satellite remote sensing products. We note that camera NDVI is not completely identical to satellite NDVI and has its own limitations. For example, camera NDVI is calculated from exposure-corrected DN values corresponding to two separate images acquired at slightly different times (e.g., 30 s apart).

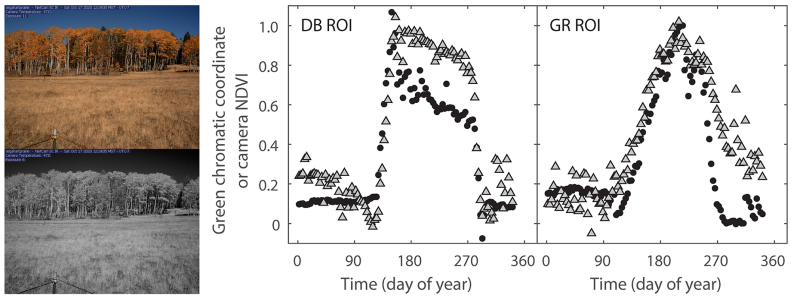

Fig. 20.5. Consecutive RGB and RGB + IR images captured using an infrared-enabled phenocam at Hart Prairie near Flagstaff, Arizona. Annual cycles of green chromatic coordinate (g_{CC} *black circles*) and camera NDVI (*gray triangles*) are plotted for ROIs corresponding to the background deciduous broadleaf forest (DB) and foreground grassland (GR). g_{CC} and NDVI have both been normalized (converted to a scale of 0–1) to enable side-by-side comparison.

áé

There are also commercially available cameras that can be used to capture continuous IR imagery. For example, Yang et al. (2017) used Tetracam's ADC (Agricultural Digital Camera) with red, green, and near-infrared channels to monitor the NDVI of a deciduous forest canopy. De Moura et al. (2017) analyzed hyperspectral imagery acquired using a tower-mounted camera to investigate changes in canopy reflectance with leaf flushing of three tropical tree species. However, there do not appear to be published studies where hyperspectral cameras have been used for continuous year-round phenological monitoring.

Finally, thermal infrared cameras that are responsive to 8–14 μm wavelengths have been used to make continuous estimates of canopy temperature (Aubrecht et al. 2016). While not directly related to monitoring phenology, such data should still be relevant to interpreting and modeling phenological processes and may provide improvements over the simplified use of air temperature in phenological studies.

20.6 Future Prospects

Much of the remote sensing technology needed for basic phenological monitoring has already been developed and to some extent made commercially available. The development of low-cost alternatives that are available in accessible packaging would help expand established technologies to an even wider user audience, while also facilitating new science applications. Even a low-cost alternative to relatively affordable (but not completely inexpensive) digital cameras would be beneficial. One solution might be something along the lines of a Raspberry Pi camera system, which is already in use by several research groups (e.g., https://hackaday.io/project/5865-phenopi). An integrated near-surface remote sensing system that could facilitate the acquisition of many different types of data at once might be particularly valuable. For example, Kim et al. (2019) developed a "Smart Surface Sensing System" for monitoring NDVI and f_{APAR}, as well as acquiring continuous RGB imagery, at a cost of less than $250. More publicly available protocols on the best practices for instrument selection and deployment would help generate the best possible data, while expanding the number of open-source software tools would facilitate standardization of methods across studies. Lastly, advances in artificial intelligence, such as deep learning, would introduce new methods for data processing and analysis. We can think of a number of applications to phenocam imagery, including automated and objective ROI selection, filtering images taken under sub-optimal conditions, and identifying and mapping phenological stages.

áę

20.7 Conclusions

Sensor-based approaches to monitoring phenology have been widely adopted over the last decade, especially the use of inexpensive digital cameras as phenocams. Studies have been conducted in diverse ecosystems of the globe and long-term (10–20 year) datasets from many monitoring sites are now available. Continental-level observation networks have been developed and a number of open-source datasets and tools are available to facilitate a wide variety of applications. We anticipate the use of this approach to continue to grow with more accessible technology, improvements to and standardization of best practices, a wider adoption of open-science principles, and an ever-pressing need to predict shifts in phenology under global change.

Acknowledgments

ORZ was supported by the Office of the Vice President for Research, Northern Arizona University. ADR acknowledges support from the National Science Foundation, awards 1832210, 2105828, 2142144, and 2224545. The data used to draw the figures were accessed from the AmeriFlux, PhenoCam, and Harvard Forest websites, and are all publicly available. The top-left photo in Fig. 21.3 was obtained from the AmeriFlux Image Gallery.

References

Almeida J, dos Santos JA, Alberton B, Torres RDS, Morellato LPC (2014) Applying machine learning based on multiscale classifiers to detect remote phenology patterns in Cerrado savanna trees. Ecol Inform 23:49–61

Andreatta D, Bachofen C, Dalponte M, Klaus VH, Buchmann N (2023) Extracting flowering phenology from grassland species mixtures using time-lapse cameras. Remote Sens Environ 298:113835

Atkins JW, Stovall AE, Yang X (2020) Mapping temperate forest phenology using tower, UAV, and ground-based sensors. Drones 4:56

Aubrecht DM, Helliker BR, Goulden ML, Roberts DA, Still CJ, Richardson AD (2016) Continuous, long-term, high-frequency thermal imaging of vegetation: Uncertainties and recommended best practices. Agr Forest Meteorol 228:315–326

Balzarolo M, Anderson K, Nichol C, Rossini M, Vescovo L, Arriga N, Wohlfahrt G, Calvet JC, Carrara A, Cerasoli S, Cogliati S, Daumard F, Eklundh L, Elbers JA, Evrendilek F, Hand-cock RN, Kaduk J, Klumpp K, Longdoz B, Matteucci G, Meroni M, Montagnani L, Ourci-val JM, Sanchez-Canete EP, Pontailler JY, Juszczak R, Scholes B, Martin MP (2011) Ground-based optical measurements at European flux sites: A review of methods, instruments and current controversies. Sensors 11:7954-7981

Bolton DK, Gray JM, Melaas EK, Moon M, Eklundh L, Friedl MA (2020) Continental-scale land surface phenology from harmonized Landsat 8 and Sentinel-2 imagery. Remote Sens Environ 240:111685

Bowling DR, Logan BA, Hufkens K, Aubrecht DM, Richardson AD, Burns SP, Anderegg WRL, Blanken PD, Eiriksson DP (2018) Limitations to winter and spring photosynthesis of a Rocky Mountain subalpine forest. Agr Forest Meteorol 252:241–255

Cogliati S, Rossini M, Julitta T, Meroni M, Schickling A, Burkart A, Pinto F, Rascher U, Colombo R (2015) Continuous and long-term measurements of reflectance and sun-induced chlorophyll fluorescence by using novel automated field spectroscopy systems. Remote Sens Environ 164:270–281

Doughty CE, Goulden ML (2008) Seasonal patterns of tropical forest leaf area index and CO_2 exchange. J Geophys Res-Biogeo 113:G00B06

Eitel JU, Griffin KL, Boelman NT, Maguire AJ, Meddens AJ, Jensen J, Vierling LA, Schmiege SC, Jennewein JS (2020) Remote sensing tracks daily radial wood growth of evergreen needleleaf trees. Glob Change Biol 26:4068–4078

Eklundh L, Jin HX, Schubert P, Guzinski R, Heliasz M (2011) An optical sensor network for vegetation phenology monitoring and satellite data calibration. Sensors 11:7678–7709

Filippa G, Cremonese E, Migliavacca M, Galvagno M, Sonnentag O, Humphreys E, Hufkens, K Ryu Y, Verfaillie J, Morra di Cella U, Richardson AD (2018) NDVI derived from near-infrared-enabled digital cameras: Applicability across different plant functional types. Agr Forest Meteorol 249:275–285

Gamon JA, Huemmrich KF, Wong CY, Ensminger I, Garrity S, Hollinger DY, Noormets A, Peñuelas J (2016) A remotely sensed pigment index reveals photosynthetic phenology in evergreen conifers. P Natl Acad Sci 113:13087–13092

Gamon JA, Penuelas J, Field CB (1992) A narrow-waveband spectral index that tracks diurnal changes in photosynthetic efficiency. Remote Sens Environ 41:35–44

Gamon JA, Serrano L, Surfus JS (1997) The photochemical reflectance index: an optical indicator of photosynthetic radiation use efficiency across species, functional types, and nutrient levels. Oecologia 112:492–501

Garrity SR, Bohrer G, Maurer KD, Mueller KL, Vogel CS, Curtis PS (2011) A comparison of multiple phenology data sources for estimating seasonal transitions in deciduous forest carbon exchange. Agr Forest Meteorol 151:1741–1752

Grossmann K, Frankenberg C, Magney TS, Hurlock SC, Seibt U, Stutz J (2018) PhotoSpec: A new instrument to measure spatially distributed red and far-red Solar-Induced Chlorophyll Fluorescence. Remote Sens Environ 216:311–327

Huemmrich KF, Black TA, Jarvis PG, McCaughey JH, Hall FG (1999) High temporal resolution NDVI phenology from micrometeorological radiation sensors. J Geophys Res-Atmos 104:27935–27944

Ide R, Oguma H (2013) A cost-effective monitoring method using digital time-lapse cameras for detecting temporal and spatial variations of snowmelt and vegetation phenology in alpine ecosystems. Ecol Infor 16:25–34

Jenkins JP, Richardson AD, Braswell BH, Ollinger SV, Hollinger DY, Smith ML (2007) Refining light-use efficiency calculations for a deciduous forest canopy using simultaneous tower-based carbon flux and radiometric measurements. Agr Forest Meteorol 143:64–79

Keenan TF, Darby B, Felts E, Sonnentag O, Friedl MA, Hufkens K, O'Keefe J, Klosterman S, Munger JW, Toomey M, Richardson AD (2014) Tracking forest phenology and seasonal physiology using digital repeat photography: a critical assessment. Ecol Appl 24:1478–1489

Kim J, Ryu Y, Jiang C, Hwang Y (2019) Continuous observation of vegetation canopy dynamics using an integrated low-cost, near-surface remote sensing system. Agr Forest Meteorol 264:164–177

Klosterman ST, Hufkens K, Gray JM, Melaas E, Sonnentag O, Lavine I, Mitchell L, Norman R, Friedl MA, Richardson AD (2014) Evaluating remote sensing of deciduous forest phenology at multiple spatial scales using PhenoCam imagery. Biogeosciences 11:4305–4320

Klosterman S, Melaas E, Wang JA, Martinez A, Frederick S, O'Keefe J, Orwig DA, Wang Z, Sun Q, Schaaf C, Friedl M, Richardson AD (2018) Fine-scale perspectives on landscape phenology from unmanned aerial vehicle (UAV) photography. Agr Forest Meteorol 248:397–407

Kosmala M, Crall A, Cheng R, Hufkens K, Henderson S, Richardson AD (2016) Season Spotter: Using citizen science to validate and scale plant phenology from near-surface remote sensing. Remote Sens 8:726

Liu J, Pattey E, Admiral S (2013) Assessment of in situ crop LAI measurement using unidirectional view digital photography. Agr Forest Meteorol, 169:25–34

Liu F, Wang X, Wang C (2019) Autumn phenology of a temperate deciduous forest: Validation of remote sensing approach with decadal leaf-litterfall measurements. Agr Forest Meteorol 279:107758

Magney TS, Bowling DR, Logan BA, Grossmann K, Stutz J, Blanken PD, Burns SP, Cheng R, Garcia MA, Köhler P, Lopez S, Parazoo NC, Raczka B, Schimel D, Frankenberg C (2019) Mechanistic evidence for tracking the seasonality of photosynthesis with solar-induced fluorescence. P Natl Acad Sci 116:11640–11645

Moon M, Richardson AD, Friedl MA (2021) Multiscale assessment of land surface phenology from harmonized Landsat 8 and Sentinel-2, PlanetScope, and PhenoCam imagery. Remote Sens Environ 266:112716

Moore CE, Brown T, Keenan TF, Duursma RA, van Dijk AI, Beringer J, Culvenor D, Evans B, Huete A, Hutley LB, Maier S, Restrepo-Coupe N, Sonnentag O, Specht A, Taylor JR, van Gorsel E, Liddell MJ (2016) Reviews and syntheses: Australian vegetation phenology: new insights from satellite remote sensing and digital repeat photography. Biogeosciences 13:5085–5102

de Moura YM, Galvão LS, Hilker T, Wu J, Saleska S, do Amaral CH, Nelson BW, Lopes AP, Wiedeman KK, Prohaska N, de Oliveira RC, Machado CB, Aragão LE (2017) Spectral analysis of amazon canopy phenology during the dry season using a tower hyperspectral camera and modis observations. ISPRS J Photogramm 131:52–64

Myneni RB, Ross J, Asrar G (1989) A review on the theory of photon transport in leaf canopies. Agr Forest Meteorol, 45:1-153

Nasahara KN, Nagai S (2015) Development of an in situ observation network for terrestrial ecological remote sensing: the Phenological Eyes Network (PEN). Ecol Res 30:211-223

Petach AR, Toomey M, Aubrecht DM, Richardson AD (2014) Monitoring vegetation phenology using an infrared-enabled security camera. Agr Forest Meteorol 195:143–151

Pierrat Z, Magney T, Parazoo NC, Grossmann K, Bowling DR, Seibt U, Johnson B, Helgason W, Barr A, Bortnik J, Norton A, Maguire A, Frankenberg C, Stutz J (2022) Diurnal and seasonal dynamics of solar-induced chlorophyll fluorescence, vegetation indices, and gross primary productivity in the boreal forest. J Geophys Res-Biogeo 127:e2021JG006588

Post AK, Hufkens K, Richardson AD (2022) Predicting spring green-up across diverse North American grasslands. Agr Forest Meteorol 327:109204

Richardson AD (2019) Tracking seasonal rhythms of plants in diverse ecosystems with digital camera imagery. New Phytol 222:1742–1750

Richardson AD (2023) PhenoCam: An evolving, open-source tool to study the temporal and spatial variability of ecosystem-scale phenology. Agr Forest Meteorol 342:109751

Richardson AD, Hufkens K, Milliman T, Aubrecht DM, Chen M, Gray JM, Johnston MR, Keenan TF, Klosterman ST, Kosmala M, Melaas EK, Friedl MA, Frolking S (2018) Tracking vegetation phenology across diverse North American biomes using PhenoCam imagery. Sci Data 5:1–24

Richardson AD, Hufkens K, Milliman T, Frolking S (2018) Intercomparison of phenological transition dates derived from the PhenoCam Dataset V1. 0 and MODIS satellite remote sensing. Sci Rep 8:5679

Rogers C, Chen JM, Croft H, Gonsamo A, Luo X, Bartlett P, Staebler RM (2021) Daily leaf area index from photosynthetically active radiation for long term records of canopy structure and leaf phenology. Agr Forest Meteorol 304:108407

Ryu Y, Baldocchi DD, Verfaillie J, Ma S, Falk M, Ruiz-Mercado I, Hehn T, Sonnentag O (2010) Testing the performance of a novel spectral reflectance sensor, built with light emitting diodes (LEDs), to monitor ecosystem metabolism, structure and function. Agr Forest Meteorol 150:1597–1606

Ryu Y, Verfaillie J, Macfarlane C, Kobayashi H, Sonnentag O, Vargas R, Ma S, Baldocchi DD (2012) Continuous observation of tree leaf area index at ecosystem scale using upward-pointing digital cameras. Remote Sens Environ 126:116–125

Schädel C, Seyednasrollah B, Hanson PJ, Hufkens K, Pearson KJ, Warren JM, Richardson AD (2023) Using long-term data from a whole ecosystem warming experiment to identify best spring and autumn phenology models. Plant Environ Interact 4:188–200

Seyednasrollah B, Bowling DR, Cheng R, Logan BA, Magney TS, Frankenberg C, Yang J, Young A, Hufkens K, Arain MA, Black TA, Blanken PD, Bracho R, Jassal R, Hollinger DY, Law BE, Nesic Z, Richardson AD (2021) Seasonal variation in the canopy color of temperate evergreen conifer forests. New Phytol 229:2586–2600

Seyednasrollah B, Young AM, Hufkens K, Milliman T, Friedl MA, Frolking S, Richardson AD (2019) Tracking vegetation phenology across diverse biomes using Version 2.0 of the PhenoCam Dataset. Sci Data 6:222

Sonnentag O, Hufkens K, Teshera-Sterne C, Young AM, Friedl M, Braswell BH, Milliman T, O'Keefe J, Richardson AD (2012) Digital repeat photography for phenological research in forest ecosystems. Agr Forest Meteorol 152:159–177

Soudani K, Delpierre N, Berveiller D, Hmimina G, Pontailler JY, Seureau L, Vincent G, Dufrêne É (2021) A survey of proximal methods for monitoring leaf phenology in temperate deciduous forests. Biogeosciences 18:3391–3408

Soudani K, Hmimina G, Delpierre N, Pontailler J-Y, Aubinet M, Bonal D, Caquet B, de Grandcourt A, Burban B, Flechard C, Guyon D, Granier A, Gross P, Heinesh B, Longdoz B, Loustau D, Moureaux C, Ourcival J-M, Rambal S, Saint André L, Dufrêne E (2012) Ground-based Network of NDVI measurements for tracking temporal dynamics of canopy structure and vegetation phenology in different biomes. Remote Sens Environ 123:234–245

Sparks TH, Menzel A (2002) Observed changes in seasons: An overview. Int J Climatol 22:1715-1725

Springer KR, Wang R, Gamon JA (2017) Parallel seasonal patterns of photosynthesis, fluorescence, and reflectance indices in boreal trees. Remote Sens 9:691

Toda M, Richardson AD (2018) Estimation of plant area index and phenological transition dates from digital repeat photography and radiometric approaches in a hardwood forest in the Northeastern United States. Agr Forest Meteorol 249:457–466

Toomey M, Friedl MA, Frolking S, Hufkens K, Klosterman S, Sonnentag O, Baldocchi DD, Bernacchi CJ, Biraud SC, Bohrer G, Brzostek E, Burns SP, Coursolle C, Hollinger DY, Margolis HA, McCaughey H, Monson RK, Munger JW, Pallardy S, Phillips RP, Torn MS, Wharton S, Zeri M, Richardson AD (2015) Greenness indices from digital cameras predict the timing and seasonal dynamics of canopy-scale photosynthesis. Ecol Appl 25:99–115

Tortini R, Hilker T, Coops NC, Nesic Z (2015) Technological advancement in tower-based canopy reflectance monitoring: The AMSPEC-III system. Sensors 15:32020–32030

Webb RH, Turner RM, Bowers JE, Hastings JR (2003) The changing mile revisited: an ecological study of vegetation change with time in the lower mile of an arid and semiarid region. University of Arizona Press, Tucson

Wilson TB, Meyers TP (2007) Determining vegetation indices from solar and photosynthetically active radiation fluxes. Agr Forest Meteorol 144:160–179

Wingate L, Ogée J, Cremonese E, Filippa G, Mizunuma T, Migliavacca M, Moisy C, Wilkinson M, Moureaux C, Wohlfahrt G, Hammerle A, Hörtnagl L, Gimeno C, Porcar-Castell A, Galvagno M, Nakaji T, Morison J, Kolle O, Knohl A, Kutsch W, Kolari P, Nikinmaa E, Ibrom A, Gielen B, Eugster W, Balzarolo M, Papale D, Klumpp K, Köstner B, Grünwald T, Joffre R, Ourcival J-M, Hellstrom M, Lindroth A, George C, Longdoz B, Genty B, Levula J, Heinesch B, Sprintsin M, Yakir D, Manise T, Guyon D, Ahrends H, Plaza-Aguilar A, Guan JH, Grace J (2015) Interpreting canopy development and physiology using a European phenology camera network at flux sites. Biogeosciences 12:5995–6015

Wohlfahrt G, Pilloni S, Hörtnagl L, Hammerle A (2010) Estimating carbon dioxide fluxes from temperate mountain grasslands using broad-band vegetation indices. Biogeosciences 7:683–694

Wong CY, D'Odorico P, Arain MA, Ensminger I (2020) Tracking the phenology of photosynthesis using carotenoid-sensitive and near-infrared reflectance vegetation indices in a temperate evergreen and mixed deciduous forest. New Phytol 226:1682–1695

Wong CY, Gamon JA (2015a) The photochemical reflectance index provides an optical indicator of spring photosynthetic activation in evergreen conifers. New Phytol 206:196–208

Wong CY, Gamon JA (2015b) Three causes of variation in the photochemical reflectance index (PRI) in evergreen conifers. New Phytol 206:187–195

Yang X, Shi H, Stovall A, Guan K, Miao G, Zhang Y, Zhang Y, Xiao X, Ryu Y, Lee J (2018) FluoSpec 2—an automated field spectroscopy system to monitor canopy solar-induced fluorescence. Sensors 18:2063

Yang H, Yang X, Heskel M, Sun S, Tang J (2017) Seasonal variations of leaf and canopy properties tracked by ground-based NDVI imagery in a temperate forest. Sci Rep 7:1267

Young AM, Friedl MA, Novick K, Scott RL, Moon M, Frolking S, Li X, Carrillo CM, Richardson AD (2022) Disentangling the Relative Drivers of Seasonal Evapotranspiration Across a Continental-Scale Aridity Gradient. J Geophys Res-Biogeo 127:e2022JG006916

Young AM, Friedl MA, Seyednasrollah B, Beamesderfer E, Carrillo CM, Li X, Moon M, Arain MA, Baldocchi DD, Blanken PD, Bohrer G, Burns SP, Chu H, Desai AR, Griffis TJ, Hollinger DY, Litvak ME, Novick K, Scott RL, Suyker AE, Richardson AD (2021) Seasonality in aerodynamic resistance across a range of North American ecosystems. Agr Forest Meteorol 310:108613

Zhang X, Liu L, Liu Y, Jayavelu S, Wang J, Moon M. Henebry GM, Friedl MA, Schaaf CB (2018) Generation and evaluation of the VIIRS land surface phenology product. Remote Sens Environ 216:212–229

B

D

ạó

F

G

I

N

P

S